THE JOURNAL OF BIOLOGICAL CHEMISTRY
Vol. 280, No. 13, Issue of April 1, pp. 12130–12136, 2005
Printed in U.S.A.

Modification of Permeability Transition Pore Arginine(s) by Phenylglyoxal Derivatives in Isolated Mitochondria and Mammalian Cells

STRUCTURE-FUNCTION RELATIONSHIP OF ARGININE LIGANDS*

Received for publication, November 30, 2004
Published, JBC Papers in Press, January 24, 2005, DOI 10.1074/jbc.M413454200

Milena Johans‡, Eva Milanesi§, Marina Franck‡, Christoffer Johans¶, Julius Liobikas‡, Maria Panagiotaki‖, Lucedio Greci‖, Giovanni Principato‖, Paavo K. J. Kinnunen‡, Paolo Bernardi§, Paola Costantini, and Ove Eriksson‡ ‡‡**

*From the ‡Helsinki Biophysics and Biomembrane Group, Institute of Biomedicine/Biochemistry, P.O. Box 63, University of Helsinki, Helsinki FIN-00014, Finland, the Departments of §Biomedical Sciences and **Biology, University of Padova, Padova I-35131, Italy, ¶Kibron Inc., P.O. Box 141, Helsinki FIN-00171, Finland, and the ‖Department of Materials and Earth Sciences, Polytechnic University of the Marche, Ancona I-60131, Italy*

Methylglyoxal and synthetic glyoxal derivatives react covalently with arginine residue(s) on the mitochondrial permeability transition pore (PTP). In this study, we have investigated how the binding of a panel of synthetic phenylglyoxal derivatives influences the opening and closing of the PTP. Using both isolated mitochondria and mammalian cells, we demonstrate that the resulting arginine-phenylglyoxal adduct can lead to either suppression or induction of permeability transition, depending on the net charge and hydrogen bonding capacity of the adduct. We report that phenylglyoxal derivatives that possess a net negative charge and/or are capable of forming hydrogen bonds induced permeability transition. Derivatives that were overall electroneutral and cannot form hydrogen bonds suppressed permeability transition. When mammalian cells were incubated with low concentrations of negatively charged phenylglyoxal derivatives, the addition of oligomycin caused a depolarization of the mitochondrial membrane potential. This depolarization was completely blocked by cyclosporin A, a PTP opening inhibitor, indicating that the depolarization was due to PTP opening. Collectively, these findings highlight that the target arginine(s) is functionally linked with the opening/closing mechanism of the PTP and that the electric charge and hydrogen bonding of the resulting arginine adduct influences the conformation of the PTP. These results are consistent with a model where the target arginine plays a role as a voltage sensor.

Mitochondrial permeability transition is a crucial event in many forms of cell death (1). Permeability transition is a consequence of the opening of the permeability transition pore (PTP),[1] a high conductance inner membrane channel (2, 3). The PTP is usually closed during normal cell life (4, 5) but can be triggered to open by an increase in matrix Ca^{2+} (2, 3) and by specific cell death signals such as ganglioside GD3 (6, 7) or arachidonic acid (8). Permeability transition promotes cell death by inducing a cellular bioenergetic crisis and by causing the release of mitochondrial proapoptotic proteins that activate caspases and degrade DNA (9). Opening of the PTP is inhibited by mitochondrial cyclophilin ligands, such as cyclosporin A (CsA) and sanglifehrin A (SfA) (10). In addition, the opening and closing of the PTP is modulated by adenine nucleotide carrier ligands (2, 3). Collectively, these findings have led to a model in which the PTP is formed by an interaction between the adenine nucleotide carrier (ANT), cyclophilin and the voltage-dependent anion channel (1, 11–13). The involvement of the voltage-dependent anion channel is supported by the identification of a novel selective high affinity PTP inhibitor, compound Ro 68-3400 (14). However, the recent finding that mitochondria from ANT knock-out mice, lacking both ANT isoforms, undergo CsA-sensitive permeability transition (15) suggests that ANT is not an essential component of the PTP.

Previously, we have studied PTP regulation using amino acid-specific covalent modification. Employing histidine- and cysteine-specific covalent reagents, we identified three separate sites through which matrix pH and the NADH/NAD^+ ratio can influence the opening and closing of the PTP (16, 17). Using phenylglyoxal (PGO), 4-hydroxyphenylglyoxal (OH-PGO), 2,3-butanedione, and methylglyoxal, which form stable adducts with guanidino groups, we have also detected reactive arginine residue(s) on the PTP (8, 18–21). The arginine adducts formed by methylglyoxal, PGO, and 2,3-butanedione stabilize the closed conformation of the PTP, preventing triggering signals from inducing PTP opening, whereas the arginine adduct formed by OH-PGO results in PTP opening even in the absence of triggering signals (20). This suggests that the glyoxal-reactive target arginine(s) is functionally coupled to the opening and closing mechanism of the pore (20). Interestingly, methyl-

* This work was supported by grants from the University of Helsinki Research Funds, the Sigrid Juselius Foundation, the Finska Läkaresällskapet, and the Perklén Memorial Foundation. The costs of publication of this article were defrayed in part by the payment of page charges. This article must therefore be hereby marked "*advertisement*" in accordance with 18 U.S.C. Section 1734 solely to indicate this fact.

‡‡ To whom correspondence should be addressed. Tel.: 358-9-191-25-404; Fax: 358-9-191-25-444; E-mail: ove.eriksson@helsinki.fi.

[1] The abbreviations used are: PTP, permeability transition pore; AGE, advanced glycation end product; ANT, adenine nucleotide carrier; CamOH-PGO, 3-carbomethoxy-4-hydroxyphenylglyoxal; Cl-PGO, 4-chlorophenylglyoxal; CsA, cyclosporin A; $\Delta\Psi$, transmembrane electric potential; 2,4-diF-PGO, 2,4-difluorophenylglyoxal; F-PGO, 4-fluorophenylglyoxal; Me-PGO, 4-methylphenylglyoxal; MeO-PGO, 4-methoxyphenylglyoxal; Mor-PGO, 4-morpholinophenylglyoxal; NO-PGO, 4-nitrophenylglyoxal; OH-PGO, 4-hydroxyphenylglyoxal; PGO, phenylglyoxal; SfA, sanglifehrin A; TMRM, tetramethylrhodamine methyl ester; MALDI-TOF, matrix-assisted laser desorption ionization time-of-flight; GD3, 1-O-[O-(*N*-acetyl-α-neuraminosyl)-(2→8)-O-(*N*-acetyl-α-neuraminosyl)-(2→3)-O-β-D-galactopyranosyl-(1→4)-β-D-glucopyranosyl]-ceramide.

glyoxal is constantly formed during glucose metabolism (22). The intracellular concentration of methylglyoxal is increased during hyperglycemia, and this leads to the formation of methylglyoxal-induced protein modifications, advanced glycation end products (AGEs), which disrupt the function of target proteins (22). AGEs are involved in several pathological processes, including diabetes mellitus and cellular proliferative disorders (23). We have proposed that methylglyoxal-induced disruption of the PTP function contributes to the development of these pathological conditions (21).

Several experimental findings indicate that a decrease in the electric potential difference ($\Delta\Psi$) across the inner mitochondrial membrane leads to an increase in the probability of the PTP being open, suggesting that the PTP directly senses the $\Delta\Psi$. In isolated Ca^{2+}-primed mitochondria, a partial depolarization of the $\Delta\Psi$ is sufficient to open the PTP (24, 25). Consistently, in patch-clamping experiments of mitoplasts, the PTP is more likely to be open at low $\Delta\Psi$ (26). The mechanism for voltage sensing by voltage-dependent ion channels is based on the movement and reorientation of positively charged amino acids in the transmembrane electric field (27). Based on (i) the effect of arginine modification on PTP conformation and (ii) the exquisite sensitivity of PTP opening and closing to small structural differences between the arginine-reactive compounds, we have proposed that the arginine(s) is located on a putative voltage-sensing element of the PTP (19, 20). Covalent modification of the voltage-sensing arginines is expected to exert a large influence on sensor orientation and therefore on pore conformation. However, the resulting sensor orientation, opened or closed, is determined by an interplay between the steric and electronic properties of the resulting arginine adduct.

In this study, we have used a set of synthetic phenylglyoxal derivatives to investigate how arginine modification alters PTP function in isolated mitochondria and mammalian cells. These phenylglyoxal derivatives differ only in the functional groups attached to the 2-, 3-, and/or 4-position of the phenyl ring. This allowed us to compare the specific physicochemical properties of the attached groups with their effects on PTP opening and closing. We found that arginine modification by these derivatives could lead either to induction or suppression of permeability transition. A physicochemical analysis revealed that negative charge and/or an ability to form hydrogen bonds was a common property of phenylglyoxal derivatives that induced permeability transition. Incubation of mammalian cells with negatively charged phenylglyoxal derivatives resulted in an increased probability of the PTP being open, and this correlated with a decrease in cell viability. These findings are consistent with a model where the target arginine(s) plays a role in the PTP voltage sensing and indicate that covalent arginine modification can affect the regulation of the PTP in intact cells.

EXPERIMENTAL PROCEDURES

Chemicals and Reagents—The structural formulas of the phenylglyoxal derivatives used in this study are shown in Fig. 1. OH-PGO and MeO-PGO were synthesized from 4-hydroxyacetophenone and 4-methoxyacetophenone by oxidation with selenium dioxide (28). Identification of the reaction product was performed using ^{1}H NMR and ^{13}C NMR spectra. NO-PGO and Fluo-4FF were purchased from Molecular Probes, Inc. (Eugene, OR). CamOH-PGO, Cl-PGO, 2,4-diF-PGO, F-PGO, Me-PGO, and Mor-PGO were from SynChem. CsA and SfA were gifts from Novartis. All other chemicals were purchased from Sigma except where otherwise noted.

Chemical Reactivity of Phenylglyoxal Derivatives with Arginine—The chemical reactions of PGO and OH-PGO with *N*-acetylarginine and peptidylarginine have been characterized (29, 30). No information is available about the reaction products formed between peptidylarginine and the following phenylglyoxal derivatives: Me-PGO, F-PGO, Cl-PGO, CamOH-PGO, 2,4-diF-PGO, Mor-PGO, and NO-PGO. Using a set of synthetic test peptides (NRVYIHPFHL, NRVYIHPF, RVYVHPF, and YGGFMRF), we investigated whether these phenylglyoxal derivatives can react covalently with the guanidine moiety of peptidylarginine. To induce the formation of the arginine adduct, 100 μM test peptide was allowed to react with 2 mM of phenylglyoxal derivative in 10 mM Hepes-KOH, pH 8.0, for 60 min at room temperature. The reaction was stopped by the addition of trifluoroacetic acid and cooling to +4 °C. The reaction mixture was desalted using a Zip Tip C18 silica bead microcolumn (Millipore Corp.). Peptides were eluted with 60% acetonitrile in 0.1% trifluoroacetic acid and mixed with an equal volume of saturated α-hydroxycyanocinnamic acid in 33% acetonitrile in 0.1% trifluoroacetic acid. MALDI-TOF mass spectra of the peptides were recorded on a Bruker Autoflex spectrometer using the reflective detector in positive mode. Calibration of the spectrometer was performed using the peaks of peptides with known masses. All of the tested phenylglyoxal compounds reacted with the peptide YGGFMRF, resulting in the formation of stable products (Fig. 2). The molecular masses of the products indicated that the phenylglyoxal derivatives were bound to the arginine residue through imidazole formation. These phenylglyoxal derivatives also reacted with the other three test peptides in a similar way.

Physicochemical Properties of Phenylglyoxal Derivatives—Dipole moments were calculated from equilibrium geometry using standard semiempiric AM1 wave functions provided in GAMESS (31). Log *P* values were calculated for the nonionic species using KowWin version 1.67 (www.syrres.com/esc/est_kowdemo.htm). The surface activity profiles of the phenylglyoxal derivatives (the surface tension *versus* concentration isotherms) were measured in modification medium containing 250 mM sucrose, 10 mM succinate, 10 mM Hepes-KOH, pH 8.0, 100 μM EGTA, 1 μM rotenone, supplemented with 10% Me_2SO, using a Delta-8 instrument (Kibron Inc.) as described (32). The apparent air/water partition coefficient was determined from the isotherms as described (32). The pK_a of the OH group of OH-PGO and CamOH-PGO was 7.50 and 7.15, respectively, as determined by the absorbance spectra of the protonated (λ_{max} at 282 and 278 nm) and deprotonated (λ_{max} at 335 and 333 nm) molecules. Titration was performed with 1 M NaOH in assay medium containing 250 mM sucrose, 10 mM Hepes-Tris, pH 7.4, 5 mM succinate, 5 mM P_i-Tris, 2 mM Mg^{2+}, 5 μM EGTA, 1 μM rotenone, supplemented with 20 mM phosphorous acid.

Isolation of Mitochondria—Liver mitochondria from male Wistar rats were prepared as described (18). The freshly isolated mitochondria (1 mg of protein/ml) were preincubated in modification medium with or without the individual phenylglyoxal derivatives for 15 min at +25 °C. The modification reaction was terminated by adjusting the pH to 6.8 with Hepes buffer and cooling to +4 °C. Mitochondria were separated from the reaction mixture containing residual free reagent by centrifugation at 8000 × *g* for 5 min. Mitochondria were resuspended at a concentration of 50 mg of protein/ml in assay medium. Sequential modification experiments were performed as described (20).

Assessment of Permeability Transition in Isolated Mitochondria—Permeability transition was induced either by a single addition of 60 μM Ca^{2+} or by repeated additions of 15 μM Ca^{2+} until fast Ca^{2+} release ensued. Permeability transition was assayed by measuring Ca^{2+} transport, mitochondrial swelling, and $\Delta\Psi$. Medium [Ca^{2+}] was measured using the fluorescent indicator dye Fluo-4FF, which becomes fluorescent upon Ca^{2+} binding (excitation, 494 nm; emission, 516 nm). Mitochondrial swelling was measured as a decrease in turbidity at 540 nm. $\Delta\Psi$ was indirectly measured by TMRM accumulation, which is sensitive to the transmembrane potential (excitation, 550 nm; emission, 575 nm). Measurements were performed using a PerkinElmer Life Sciences LS50B luminescence spectrometer. PTP opening was quantified by the swelling rate and Ca^{2+} threshold, as described (21, 33).

Cell Culture—MH1C1 rat hepatoma cells were grown in Ham's F-10 (Invitrogen) nutrient mixture supplemented with 40 mM $NaHCO_3$, 10% fetal calf serum, 30 μg/ml penicillin, and 50 μg/ml streptomycin. HeLa cells were grown in Dulbecco's modified Eagle's medium (Invitrogen) medium supplemented with 2 mM glutamine, 10% fetal calf serum, 30 μg/ml penicillin, and 50 μg/ml streptomycin. Cells were kept at +37 °C in a humidified atmosphere containing 5% CO_2. To induce arginine modification, cells were incubated in a culture medium supplemented with the phenylglyoxal derivatives for 12 h. The remaining derivative was removed from the culture medium after the incubation, and cell viability was assessed using the resazurin assay according to the manufacturer's instructions. After 3 h, the ratio of reduced to oxidized resazurin was measured using a microplate reader (Spectracount; Packard) at the wavelength couple 620–540 nm.

Microscopy—For light microscopy, cells were seeded onto glass coverslips in 6-well plates and incubated overnight. The coverslips were mounted on the stage of a Zeiss Axiovert 100TV inverted microscope equipped with a mercury lamp (100 watts). $\Delta\Psi$ was measured using the

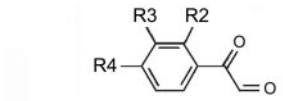

	R4	R3	R2
PGO	-	-	-
Me-PGO	-CH_3	-	-
MeO-PGO	-O-CH_3	-	-
F-PGO	-F	-	-
2,4-diF-PGO	-F	-	-F
3,4-diF-PGO	-F	-F	-
Cl-PGO	-Cl	-	-
NO-PGO	$-N^{+}(O^{-})=O$	-	-
OH-PGO	$-O^{-}$	-	-
CamOH-PGO	$-O^{-}$	$-C(=O)-O-CH_3$	-
Mor-PGO	$-N$ (morpholine)	-	-

FIG. 1. **Structural formulas of phenylglyoxal derivatives.** For clarity, hydrogen atoms (-H) on the phenyl ring are not shown. The pK_a of the OH group of OH-PGO and CamOH-PGO was 7.50 and 7.15, respectively.

fluorescent indicator dye TMRM. The excitation filter wavelength was 546 ± 5 nm, the emission filter wavelength was 580 ± 15 nm, and the dichroic mirror cut-off wavelength was 560 nm. Images were acquired using a 12-bit CCD camera and analyzed using the MetaFluor imaging software (Micromax; Princeton Instruments). Before the measurement, cells were incubated for 30 min at +37 °C in Hanks' balanced salt solution (Sigma) supplemented with 20 nM TMRM and 1.6 μM cyclosporin H. Unlike CsA, cyclosporin H does not inhibit the PTP, whereas both compounds inhibit the multidrug resistance pump, and therefore cyclosporin H was used to optimize TMRM loading as detailed (34). Mitochondrial clusters were defined as regions of interest, and background fluorescence was measured from fields without cells. Sequential digital images were acquired every 0.5–2 min for 60 min, and the average fluorescence intensity of all of the selected regions of interest and of the background was recorded and stored for subsequent analysis.

RESULTS

To investigate the structure-function relationship of arginine-glyoxal adducts upon PTP opening and closing, we used a set of phenylglyoxal derivatives that differ only in the functional groups attached to the phenyl ring (Fig. 1). All of these phenylglyoxal derivatives can react with peptidylarginine and form stable adducts as evidenced by the molecular mass of the resulting reaction products (Fig. 2). We then investigated the effects of the phenylglyoxal derivatives on the PTP in isolated rat liver mitochondria, and Fig. 3 shows our findings with Me-PGO. Mitochondria were incubated with or without 2 mM Me-PGO and subsequently resuspended in assay medium, and permeability transition was induced by a single addition of 60 μM Ca^{2+}. Control mitochondria that had been incubated without Me-PGO took up Ca^{2+} from the medium (Fig. 3*A*, *trace a*). The addition of Ca^{2+} to the assay medium can be seen as an increase in the Fluo-4FF fluorescence at 2 min. As the control mitochondria took up the added Ca^{2+}, the Fluo-4FF fluorescence decreased. However, these mitochondria subsequently released Ca^{2+} back into the medium and underwent large amplitude swelling as indicated by the large decrease in turbidity (Fig. 3, *A* and *B*, *traces a*). Concomitantly, the ΔΨ diminished (Fig. 3*C*, *trace a*), indicating that deenergization had occurred. Supplementing the assay medium of control mitochondria with 1 μM CsA (Fig. 3, *all panels*, *traces b*) or SfA (data not shown) completely inhibited Ca^{2+} release, swelling, and the ΔΨ decrease, indicating that these events were due to PTP

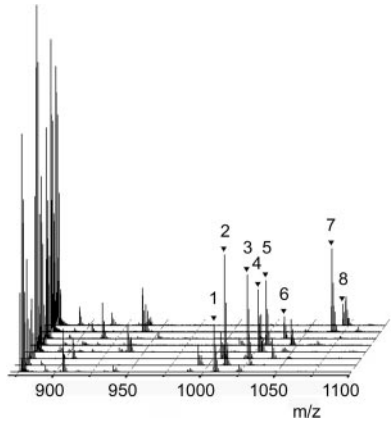

FIG. 2. **MALDI-TOF mass spectra of phenylglyoxal derivatives bound to a test peptide.** The peptide (YGGFMRF) was reacted with each phenylglyoxal derivative as described under "Experimental Procedures." The reaction mixture was desalted and applied to the target. Mass spectra were acquired in the positive mode using the reflective detector. The phenylglyoxal derivatives used were as follows. *1*, Me-PGO; *2*, F-PGO; *3*, MeO-PGO; *4*, Cl-PGO; *5*, 2,4-diF-PGO, *6*, NO-PGO; *7*, CamOH-PGO; *8*, Mor-PGO. The peak at *m/z* 877.40 in the spectra is due to remaining underivatized peptide.

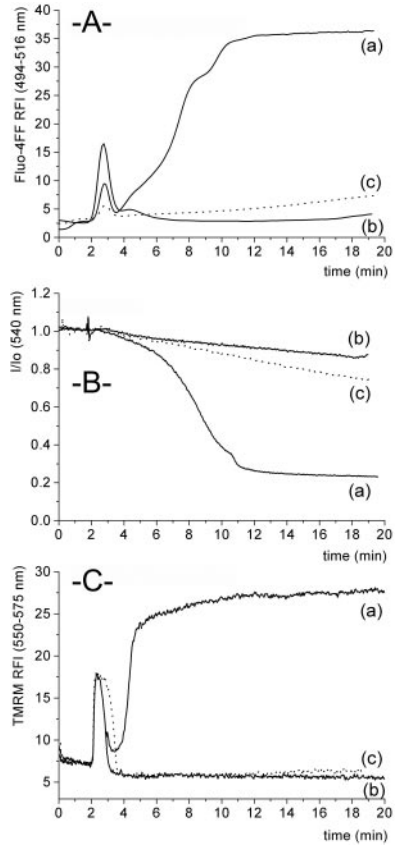

FIG. 3. **Inhibition of Ca^{2+}-induced PTP opening by Me-PGO.** Mitochondria were preincubated for 15 min with or without 2 mM Me-PGO. Mitochondria were then sedimented by centrifugation and resuspended in assay medium at a concentration of 1 mg of protein/ml. Ca^{2+} (60 μM) was added after 2 min. *A*, Ca^{2+} concentration of the medium measured using the fluorescent dye Fluo-4FF. *B*, swelling measured as a decrease in turbidity. *C*, ΔΨ measured using the fluorescent dye TMRM. *All panels*, *traces a* and *b* show mitochondria preincubated without Me-PGO; *traces c* show Me-PGO-treated mitochondria; in *traces b*, the suspension was supplemented with 1 μM CsA.

opening. In contrast, mitochondria that had been incubated with Me-PGO were able to retain the added Ca^{2+} in the matrix throughout the experiment (Fig. 3*A*, *trace c*). Me-PGO-treated

TABLE I

Effect of phenylglyoxal derivatives on the PTP and their physicochemical properties

Mitochondria were incubated with the derivatives, and the effect on the PTP was quantified by the mitochondrial swelling rate and Ca^{2+} uptake threshold. The physicochemical properties were determined as described under "Experimental Procedures."

Compound	Swelling rate[a]	Ca^{2+} threshold[a]	Dipole moments (*D*)				Log *P*	Apparent log K_{aw}/M	Hydrogen bond donor	Hydrogen bond acceptor
			x	*y*	*z*	Total				
	%	%								
PGO	12	487	−2.1	0.0	−4.2	4.7	1.0	3.0	No	No
Me-PGO	14	350	2.1	0.0	4.7	5.2	1.5	2.7	No	No
MeO-PGO	36	183	0.8	0.0	2.4	2.5	1.0	2.2	No	Weak
F-PGO	12	550	−2.0	0.0	−2.7	3.3	1.2	ND[b]	No	No
2,4-diF-PGO	32	250	3.1	0.0	−3.2	4.4	1.4	2.7	No	No
Cl-PGO	25	237	−2.0	0.0	−2.9	3.5	1.6	2.4	No	No
NO-PGO	300	15	1.6	0.0	1.2	2.0	0.8	2.2	No	Yes
OH-PGO	430[c]	18[c]	−0.9	0.0	4.2	4.3	0.5	1.6	Yes	Yes
(O^-)-PGO	430[c]	18[c]	−2.6	0.0	−2.2	3.4	ND[d]		Yes	Yes
CamOH-PGO	550[c]	18[c]	−1.0	0.1	−2.0	2.2	1.6	2.3	Yes	Yes
Cam(O^-)-PGO	550[c]	18[c]	0.1	−2.0	3.5	4.1	ND[d]		Yes	Yes
Mor-PGO	100	100	0.0	−3.2	2.0	3.8	0.7	2.1	No	Yes
CsA/SfA	<5	>450								
Control	100	100								

[a] Since the sensitivity of the PTP to Ca^{2+} can vary between different mitochondrial preparations, the swelling rate and Ca^{2+} threshold are expressed in relative values as described under "Experimental Procedures."

[b] Not determined.

[c] Determined for the prevailing equilibrium between the protonated and deprotonated form at pH 7.4.

[d] Log *P* not defined for ions.

mitochondria remained energized, and swelling did not occur as indicated by the unchanged turbidity of the mitochondrial suspension (Fig. 3, *all panels*, *traces c*). These results show that brief Me-PGO treatment results in suppression of permeability transition. Since Me-PGO had no detrimental effect on the generation of $\Delta\Psi$ or Ca^{2+} uptake, we conclude that Me-PGO acted directly on the PTP.

The results of similar measurements on isolated mitochondria incubated with the other phenylglyoxal derivatives are summarized in Table I. For comparison, we included data on PGO and OH-PGO (19, 20). In order to quantify the PTP opening/closing, we also determined the Ca^{2+} uptake threshold for PTP opening as described (33). To illustrate how Ca^{2+} uptake threshold measurements were performed, we show results for mitochondria incubated with either Me-PGO (Fig. 4*A*) or CamOH-PGO (Fig. 4*B*). After removal of excess phenylglyoxal derivative, mitochondria were suspended in the assay medium as described above, and pulses of 15 μM Ca^{2+} were added until Ca^{2+} release ensued. The results showed that mitochondria incubated without phenylglyoxal derivative (Fig. 4, *A* and *B*, *traces a*) were able to take up about 55 nmol of Ca^{2+}/mg of protein from the medium before Ca^{2+} release occurred, whereas treatment with Me-PGO (Fig. 4*A*, *trace b*) increased the Ca^{2+} uptake threshold to 190 nmol of Ca^{2+}/mg of protein. Supplementing the medium of control mitochondria with 1 μM CsA or SfA increased the Ca^{2+} uptake threshold to over 200 nmol of Ca^{2+}/mg of protein (data not shown). Therefore, Me-PGO treatment of mitochondria resulted in a 4-fold increase in the Ca^{2+} threshold, showing that Me-PGO was almost as effective as the cyclophilin ligands for closing the PTP. In contrast, incubation with CamOH-PGO resulted in a dramatic decrease in the Ca^{2+} threshold. In this case, one single pulse of 15 μM Ca^{2+} was sufficient to trigger Ca^{2+} release, compared with the four pulses for mitochondria incubated without phenylglyoxal derivative (Fig. 4*B*, *traces a* and *b*). The Ca^{2+} release from mitochondria incubated with CamOH-PGO remained fully sensitive to both 1 μM CsA and SfA (Fig. 4*B*, *traces c* and *d*). This result demonstrates that CamOH-PGO acts selectively on the PTP and increases the likelihood of PTP opening in response to Ca^{2+}. During incubation of isolated mitochondria with the phenylglyoxal derivatives CamOH-PGO, OH-PGO, and NO-PGO, energization by

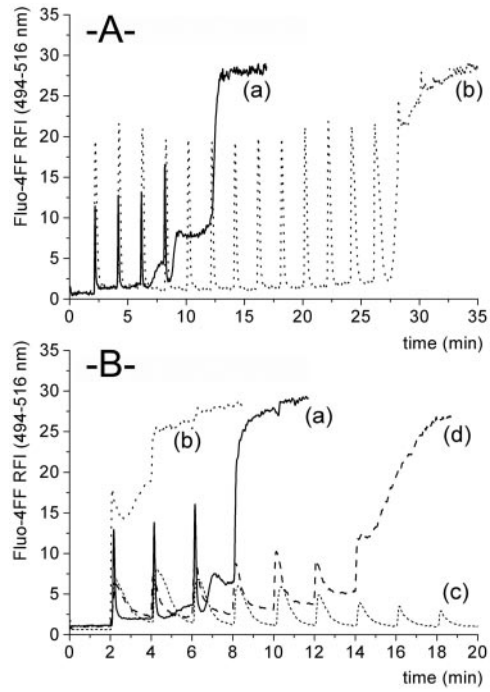

FIG. 4. **Effect on mitochondrial Ca^{2+} uptake threshold by Me-PGO and CamOH-PGO.** Mitochondria were preincubated with 2 mM Me-PGO (*A*) or 2 mM CamOH-PGO (*B*). Ca^{2+} transport was measured as in Fig. 3*A*. Ca^{2+} (15 μM) was added every other minute. *Both panels*, *traces a* show control mitochondria preincubated without phenylglyoxal derivative. *A*, *trace b* shows mitochondria preincubated with Me-PGO; *B*, *traces b–d* show mitochondria preincubated with CamOH-PGO. The medium was supplemented with 1 μM CsA in *trace c* and with 1 μM SfA in *trace d*.

succinate was required to prevent spontaneous permeability transition (data not shown). Comparing the results of the phenylglyoxal derivatives, it is evident that rapid mitochondrial swelling correlated with a low Ca^{2+} uptake threshold, and *vice versa*. None of the phenylglyoxal derivatives had any major effects on the generation of $\Delta\Psi$ or Ca^{2+} uptake at concentrations that effectively modify the PTP (data not shown).

The phenylglyoxal derivatives can be categorized into three

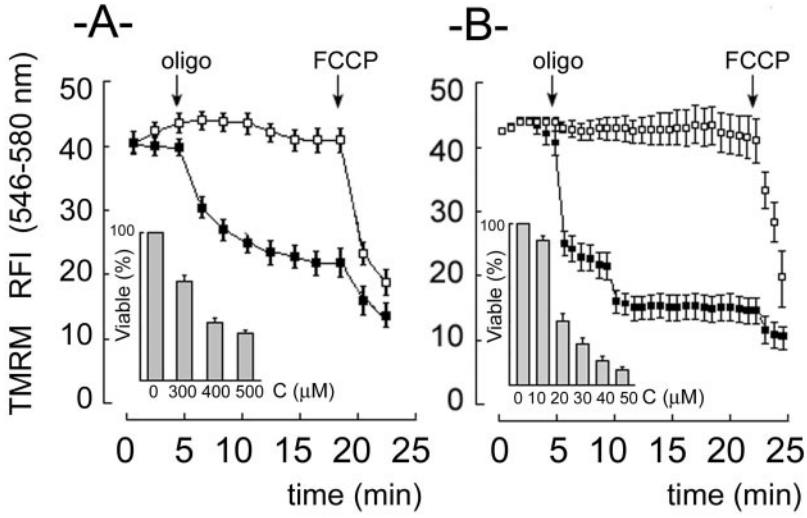

FIG. 5. **Effect of OH-PGO and CamOH-PGO on permeability transition and viability in mammalian cells.** Cells were incubated with phenylglyoxal derivatives for 12 h as described under "Experimental Procedures." $\Delta\Psi$ was measured using TMRM (*main graphs*), and cell viability was assessed using the resazurin assay (*insets*). *A*, *main graph,* MH1C1 cells incubated with 300 μM OH-PGO. *B*, *main graph*, HeLa cells incubated with 20 μM CamOH-PGO. The addition of 2 μg/ml oligomycin and 2 μM carbonyl cyanide *p*-trifluoromethoxyphenylhydrazone (*FCCP*) are indicated with *arrows*. *Open squares* indicate that 1 μM CsA was added immediately before the measurement. *A*, *inset*, the relationship between OH-PGO concentration and the survival of MH1C1 cells. *B*, *inset*, the relationship between CamOH-PGO concentration and the survival of HeLa cells.

groups: (i) those that suppressed permeability transition (Cl-PGO, 2,4-diF-PGO, F-PGO, Me-PGO, MeO-PGO, and PGO); (ii) those that induced permeability transition (CamOH-PGO, NO-PGO, and OH-PGO); and (iii) one (Mor-PGO) that had no effect on permeability transition. Similar to CamOH-PGO-induced PTP opening, NO-PGO- and OH-PGO-induced PTP opening was inhibited by CsA or SfA (data not shown). To understand why Mor-PGO did not influence the PTP conformation, we conducted a sequential modification experiment. Mitochondria were incubated with PGO, sedimented by centrifugation, and resuspended in Mor-PGO-containing medium. Subsequently, the mitochondria were sedimented and resuspended in assay medium. Alternatively, we first incubated with Mor-PGO and then with PGO. We then determined how these two treatment schemes affected the PTP, as in Fig. 3. The results showed that PTP closing occurred, regardless of whether PGO was used before or after Mor-PGO (data not shown), indicating that Mor-PGO did not react with the target arginine(s).

We then analyzed the physicochemical properties of the phenylglyoxal derivatives and compared these properties with their effects on the PTP (Table I). This analysis revealed that OH-PGO and CamOH-PGO, which are partially protonated and thus negatively charged at neutral pH, are PTP-openers. We calculated the dipole moment (*D*) and the octanol/water partition coefficients (log *P*) and measured the surface activity profile (apparent log K_{aw}/M), which provides an alternative to log *P* for characterizing the lipophilicity or amphiphilicity of a compound, particularly in anisotropic environments (32, 35, 36). None of these parameters showed any significant correlation with the PTP opening/closing data, indicating that the effect cannot be predicted based on hydrophobicity/lipophilicity or dipole moment. Finally, we examined the hydrogen bonding capacity of the side chain groups. The hydrogen bonding properties have been classified as either hydrogen bond donors or acceptors. This analysis showed that the PTP openers CamOH-PGO, OH-PGO, and NO-PGO can form hydrogen bonds. In contrast, the PTP closers Cl-PGO, 2,4-diF-PGO, F-PGO, Me-PGO, and PGO do not form hydrogen bonds. The only exception to this general rule is MeO-PGO. However, MeO-PGO is a very weak hydrogen bond acceptor (37), and apparently this property is not sufficient to induce PTP opening. Our analysis therefore revealed that negative charge and hydrogen bonding capacity is a common property of the PTP openers.

We then investigated the effect of the phenylglyoxal derivatives on the PTP in mammalian cells. It must be considered that incubation of mammalian cells with these compounds may have toxic effects, independently of how they affect the PTP. In the case of the PTP closers (Cl-PGO, 2,4-diF-PGO, F-PGO, Me-PGO, MeO-PGO, and PGO), this leads to a complex situation where their general cellular toxicity may mask their effects on the PTP. The situation is more straightforward for PTP openers (CamOH-PGO, NO-PGO, and OH-PGO), since both PTP opening and general toxicity promote cell death and therefore the involvement of the PTP can be assessed through the protective effects of CsA. Based on these considerations, we limited this study to PTP openers. First, we determined the optimal phenylglyoxal derivative concentration for the study using the viability resazurin assay. Incubation of rat hepatoma MH1C1 cells with OH-PGO for 12 h reduced the number of viable cells, and the LD_{50} value was 300 μM (Fig. 5*A*, *inset*), which we chose as the concentration to study PTP triggering. After washing of the cells and TMRM loading, the $\Delta\Psi$ was monitored under the epifluorescence microscope (Fig. 5*A*, *main graph*). When cells were incubated with OH-PGO, the addition of the ATPase inhibitor oligomycin induced a rapid decrease in TMRM fluorescence indicating $\Delta\Psi$ depolarization. This depolarization was completely prevented by supplementing the culture medium with CsA, indicating that the depolarization was due to PTP opening. CsA was effective even when added immediately before oligomycin, showing that the OH-PGO treatment resulted in a sensitization of the PTP. As expected, the addition of the protonophore carbonyl cyanide *p*-trifluoromethoxyphenylhydrazone to OH-PGO treated in cells supplemented with CsA resulted in a complete depolarization of the $\Delta\Psi$. The $\Delta\Psi$ in OH-PGO-treated and untreated control cells were similar to each other (results not shown). There was no effect of oligomycin on the $\Delta\Psi$ in untreated control cells (results not shown). This finding demonstrates that OH-PGO treatment induces cell death, which is preceded by an increased probability of the PTP being open, suggesting that OH-PGO had formed an adduct on the target PTP arginine(s). We then investigated the effect of NO-PGO and CamOH-PGO. The LD_{50} values for these derivatives is about 10 μM (data not shown). However, at this concentration, neither NO-PGO nor CamOH-

PGO was able to increase the probability of PTP opening, as judged by the lack of effects by oligomycin on the $\Delta\Psi$ (data not shown). These findings show that inhibition of the ATPase did not reveal a latent PTP sensitization, suggesting that NO-PGO- and CamOH-PGO-induced cell death was not preceded by an increased probability of the PTP being open.

To assess whether the effects of the phenylglyoxal derivatives were cell-specific, we also studied their effects upon human cervical carcinoma HeLa cells. Interestingly, we found that CamOH-PGO, but neither OH-PGO nor NO-PGO, was able to induce PTP opening. Following incubation of HeLa cells at an LD_{50} of 20 μM CamOH-PGO (Fig. 5*B*, *inset*), the $\Delta\Psi$ depolarized upon the addition of oligomycin (Fig. 5*B*, *main graph*), and this effect could be completely prevented by adding CsA. Incubation at low concentrations ($\ll LD_{50}$) of OH-PGO, CamOH-PGO, or NO-PGO had no measurable effects on the PTP in MH1C1 or HeLa cells (data not shown). Taken together, these findings are consistent with the effects of OH-PGO and CamOH-PGO on isolated mitochondria and show that the PTP is a potentially important target for glyoxal derivatives in mammalian cells.

DISCUSSION

In this study, we have used a set of phenylglyoxal derivatives to investigate the effect of arginine modification on PTP opening and closing in isolated mitochondria and mammalian cells. Analysis of the structure-function relationship showed that negative charge and hydrogen bonding capacity was a common property of derivatives that induced PTP opening. We conclude that glyoxal compounds can regulate the PTP in intact cells and that this may lead to a disruption of the cell death program.

Using a series of test peptides, we demonstrated that all of the phenylglyoxal derivatives studied formed stable adducts on the arginine side chain. Thus, neither steric nor electronic factors of the different functional groups perturb the reaction between the glyoxal and the guanidino groups. Ensuring that our phenylglyoxal derivatives react with peptidylarginine was an essential prerequisite before studying their effects on PTP opening and closing. In isolated mitochondria, all of the phenylglyoxal derivatives except Mor-PGO had an effect on the PTP after a relatively short incubation time, showing that the functional groups in the 2-, 3-, and/or 4-position of the phenyl ring do not compromise the ability of the phenylglyoxal compounds to bind to the target PTP arginine(s). However, despite the reactivity of Mor-PGO with the test peptides, Mor-PGO did not react with the PTP target arginine(s), suggesting that the reaction was hindered by its bulky side chain (Fig. 1). Since none of the phenylglyoxal derivatives had detrimental effects on the generation of $\Delta\Psi$ or Ca^{2+} uptake, we conclude that they acted directly upon the PTP. Therefore, the finding that some phenylglyoxal derivatives (Cl-PGO, 2,4-diF-PGO, F-PGO, Me-PGO, MeO-PGO, and PGO) promote PTP closing, whereas others (CamOH-PGO, NO-PGO, and OH-PGO) induce PTP opening, can be explained by the differences in the physicochemical properties of the functional groups.

Properties that influence the microenvironment around the target arginine(s) include electrical charge, dipole moment, polarity, and hydrogen bonding of the neighboring chemical groups. We found that OH-PGO and CamOH-PGO, which carry a net negative charge and can participate in hydrogen bonding, were PTP openers. In addition, NO-PGO, which can form hydrogen bonds but carries no net charge also induced PTP opening. We found that Cl-PGO, 2,4-diF-PGO, F-PGO, Me-PGO, and PGO, which have electroneutral side chains that do not form hydrogen bonds, close the PTP. Interestingly, we found that MeO-PGO, which is electroneutral, closed the PTP. However, MeO-PGO is a weak hydrogen bond acceptor, and this property can explain why MeO-PGO was the least potent of the PTP closing compounds. No correlation could be found between dipole moment, partition coefficient, or surface activity and effects on the PTP. However, the polarity values for all of the phenylglyoxal derivatives are within a narrow range, and therefore they are unlikely to contribute to the observed differences. Collectively, the observations of the present study indicate that the critical adduct properties are net electric charge and hydrogen bonding capacity.

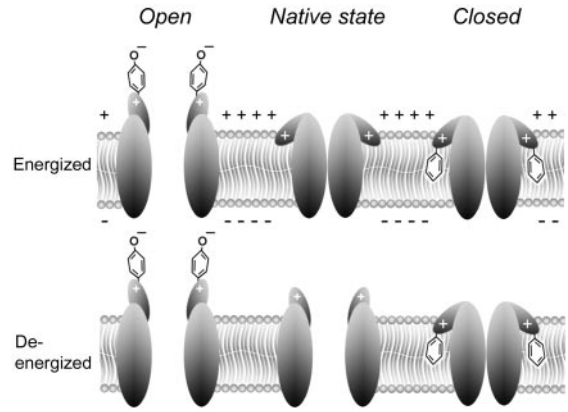

FIG. 6. **Hypothetical model of the PTP gating.** The native state of the PTP is shown in the *middle*. The voltage sensor, shown as *two paddles* on the external part of the pore, is able to reorientate according to the direction and strength of the electric field. At high $\Delta\Psi$, the positively charged sensor is pulled into the low dielectric membrane interior by the electric field. This orientation favors a closed pore conformation (*upper row*). Upon depolarization of the $\Delta\Psi$, the voltage sensor moves out of the membrane interior and is located in the aqueous phase forming hydrogen bonds. This orientation favors an open pore conformation (*lower row*). A negatively charged and/or hydrogen bond-forming arginine adduct would keep the voltage sensor in the aqueous phase irrespective of the magnitude of the $\Delta\Psi$ (*left*). This stabilizes an open pore conformation. An electroneutral and non-hydrogen bond-forming adduct would stabilize the position of the sensor inside the low dielectricity membrane interior irrespective of the magnitude of the $\Delta\Psi$ (*right*). This stabilizes a closed pore conformation. This model is based on the gating mechanism proposed by Jiang *et al.* (38).

Although the structure of the PTP remains unsolved, our results support a simple model for a voltage-dependent pore gate (Fig. 6). In voltage-dependent ion channels, positively charged amino acid residues play a key role in translating changes in membrane potential to conformational changes of the ion pore (27). We propose a PTP model based on the "voltage paddle" mechanism similar to that of the voltage-gated K^+ channel (38). The reactive arginine is assigned to a hypothetical loop or helix protruding from the external channel surface, the orientation of which determines the conformation of the pore. In the absence of any arginine adduct, the arginine-containing loop reorientates according to the magnitude of the $\Delta\Psi$. At high $\Delta\Psi$, the loop would be pulled by the electric field into the low dielectric environment, resulting in a closed pore conformation. Upon depolarization of the $\Delta\Psi$, the arginine-containing loop would reorientate into the aqueous environment, reforming hydrogen bonds and inducing a transition of the pore to an open conformation. Modification of the arginine with a negatively charged or hydrogen bond-forming phenylglyoxal derivative would result in charge neutralization and formation of hydrogen bonds in the aqueous environment. This would cause an increase in the energy barrier that must be overcome for moving the loop back into the membrane interior at high $\Delta\Psi$ and therefore result in a stabilization of an open pore conformation. In contrast, modification of the arginine(s) with an electroneutral non-hydrogen-bonding derivative would shield the positive charge and reduce the number of hydrogen bonds formed in the aqueous

environment. This would make the intramembrane orientation of the loop energetically more favorable at low $\Delta\Psi$ and result in a stabilization of a closed pore conformation.

It is clear from our work that glyoxal compounds have major effects on the function of the PTP in isolated mitochondria. However, the regulation of the PTP in intact cells may differ from that of isolated mitochondria. Therefore, we addressed whether the PTP target arginine(s) is modified by phenylglyoxal derivatives in intact mammalian cells. The partition coefficient and surface activity profiles suggested that the phenylglyoxal derivatives are cell membrane-permeable. However, several factors may affect the fate of the derivative when it reaches the cell interior. These include (i) the presence of additional potential targets and (ii) metabolic conversion, which may be different in different cell lines. Of particular concern is aromatic hydroxylation, which would turn a PTP closer (PGO) to a PTP opener (OH-PGO) (39). Therefore, these factors may explain the cell-specific response to different phenylglyoxal derivatives.

AGEs play a key role in the molecular mechanism of long term complications of diabetes (23). The most important intracellular precursor of AGEs is methylglyoxal, which reacts preferentially with arginine residues, causing altered function of target proteins (22). Small amounts of methylglyoxal are constantly formed as a side product from the reaction catalyzed by triose-phosphate isomerase (40), a process that is greatly accelerated during hyperglycemia, leading to an increased formation of AGEs. Since the PTP arginine(s) is responsive to phenylglyoxal compounds in intact cells, it is possible that the PTP is a target for methylglyoxal and/or its metabolic products. Experiments aimed at testing this hypothesis are under way in our laboratory.

Acknowledgments—We thank Michael Verkhovsky for critical reading of the manuscript and Kaija Niva for excellent technical assistance.

REFERENCES

1. Kim, J -S., He, L., and Lemasters, J. J. (2003) *Biochem. Biophys. Res. Commun.* **304,** 463–470
2. Zoratti, M., and Szabo, I. (1995) *Biochim. Biophys. Acta* **1241,** 139–176
3. Bernardi, P. (1999) *Physiol. Rev.* **79,** 1127–1155
4. Eriksson, O., Geimonen, E., and Pollesello, P. (1999) *Am. J. Physiol.* **276,** C1297–C1302
5. Petronilli, V., Penzo, D., Scorrano, L., Bernardi, P., and Di Lisa, F. (1999) *J. Biol. Chem.* **276,** 12030–12034
6. Kristal, B. S., and Brown, A. M. (1999) *J. Biol. Chem.* **274,** 23169–23175
7. Scorrano, L., Petronilli, V., Di Lisa, F., and Bernardi P. (1999) *J. Biol. Chem.* **274,** 22581–22585
8. Scorrano, L., Penzo, D., Petronilli, V., Pagano, F., and Bernardi, P. (2001) *J. Biol. Chem.* **276,** 12035–12040
9. Van Gurp, M., Festjens, N., van Loo, G., Saelens, X., and Vandenabeele, P. (2003) *Biochem. Biophys. Res. Commun.* **304,** 487–497
10. Clarke, S. J., McStay, G. P., and Halestrap, A. P. (2002) *J. Biol. Chem.* **277,** 34793–34799
11. Desagher, S., and Martinou, J.-C. (2000) *Trends Cell Biol.* **10,** 369–377
12. Vieira, H. L., Haouzi, D., El Hamel, C., Jacotot, E., Belzacq, A. S., Brenner, C., and Kroemer, G. (2000) *Cell Death Differ.* **7,** 1146–1154
13. Halestrap, A. (2003) *Curr. Med. Chem.* **10,** 1507–1525
14. Cesura, A. M., Pinard, E., Schubenel R., Gotschy, V., Friedlein, A., Langen, H-. Polcic, P., Forte, M., Bernardi, P., and Kemp, J. A. (2003) *J. Biol. Chem.* **278,** 49812–49818
15. Kokoszka, J. E., Waymire, K. G., Levy, S. E., Sligh, J. E., Cai, J., Jones, D. P., MacGregor, G. R., and Wallace, D. C. (2004) *Nature* **427,** 461–465
16. Nicolli, A., Petronilli, V., and Bernardi, P. (1993) *Biochemistry* **32,** 4461–4465
17. Chernyak, B. V., and Bernardi, P. (1996) *Eur. J. Biochem.* **238,** 623–630
18. Eriksson, O., Fontaine, E., Petronilli, V., and Bernardi, P. (1997) *FEBS Lett.* **409,** 361–364
19. Eriksson, O., Fontaine, E., and Bernardi, P. (1998) *J. Biol. Chem.* **273,** 12669–12674
20. Linder, M. D., Morkunaite-Haimi, S., Kinnunen, P. K. J., Bernardi, P., and Eriksson, O. (2002) *J. Biol. Chem.* **277,** 937–942
21. Speer, O., Morkunaite-Haimi, S., Liobikas, J., Franck, M., Hensbo, L., Linder, M. D., Kinnunen, P. K. J., Wallimann, T., and Eriksson, O. (2003) *J. Biol. Chem.* **278,** 34757–34763
22. Thornalley, P. J. (1995) *Crit. Rev. Oncol. Hematol.* **99,** 99–128
23. Brownlee, M. (2001) *Nature* **414,** 813–820
24. Bernardi, P. (1992) *J. Biol. Chem.* **267,** 8834–8839
25. Petronilli, V., Cola, C., and Bernardi, P (1993) *J. Biol. Chem.* **268,** 1011–1016
26. Szabo, I., and Zoratti, M. (1993) *FEBS Lett.* **330,** 201–205
27. Bezanilla, F. (2000) *Physiol. Rev.* **80,** 555–592
28. Fodor, G., and Kovacs, O. (1949) *J. Am. Chem. Soc.* **71,** 1045–1049
29. Takahashi, K. (1968) *J. Biol. Chem.* **243,** 6171–6179
30. Yamasaki, R. B., Vega, A., and Feeney, R. E. (1980) *Anal. Biochem.* **109,** 32–40
31. Schmidt, M. W., Baldridge, K. K., Boatz, J. A., Elbert, S. T., Gordon, M. S., Jensen, J. H., Koseki, S., Matsunaga, N., Nguyen, K. A., Su, S. J., Windus, T. L., Dupuis, M., and Montgomery, J. A. (1993) *J. Comput. Chem.* **14,** 1347–1363
32. Suomalainen, P., Johans, C., Söderlund, T., and Kinnunen, P. K. J. (2004) *J. Med. Chem.* **47,** 1783–1788
33. Walter, L., Nogueira, V., Leverve, X., Heitz, M.-P., Bernardi, P., and Fontaine, E. (2000) *J. Biol. Chem.* **275,** 29521–29527
34. Bernardi, P., Scorrano, L., Colonna, R., Petronilli, V., and Di Lisa, F. (1999) *Eur. J. Biochem.* **264,** 687–701
35. Seelig, A., Gottschlich, R., and Devant, R. M. (1994) *Proc. Natl. Acad. Sci. U. S. A.* **91**, 68–72
36. Fischer, H., Gottschlich, R., and Seelig, A. (1998) *J. Membr. Biol.* **165,** 201–211
37. Abraham, M. H., Duce, P. P., Prior, D. V., Barratt, D. G., Morris, J. J., and Taylor, P. J. (1989) *J. Chem. Soc. Perkin Trans.* **II,** 1355–1375
38. Jiang, Y., Ruta, V., Chen, J., Lee, A., and MacKinnon, R. (2003) *Nature* **423,** 42–48
39. Guengrich, F. P. (2001) *Chem. Res. Toxicol.* **14,** 611–650
40. Pompliano, D. L., Peyman, A., and Knowles, J. R. (1990) *Biochemistry* **29,** 3186–3194